



Morphological variants of Sindbis virus produced by a mutation in the capsid protein

Davis Ferreira,¹ Raquel Hernandez, Michelle Horton, and Dennis T. Brown*

Department of Molecular and Structural Biochemistry, North Carolina State University, Raleigh, NC 27695, USA

Received 26 July 2002; returned to author for revision 2 October 2002; accepted 9 October 2002

Abstract

Sindbis virus is a complex aggregate of RNA, protein and lipid. The virus is organized as two nested $T = 4$ icosahedral protein shells between which is sandwiched a lipid bilayer. The virus RNA resides within the inner protein shell. The inner protein shell is attached to the outer protein shell through contacts to proteins in the outer shell, which penetrate the lipid bilayer. The data presented in the following manuscript show that mutations in the capsid protein can result in the assembly of the virus structural proteins into icosahedra of different triangulation numbers. The triangulation numbers calculated, for these morphological variants, follow the sequence $T = 4, 9, 16, 25$ and 36 . All fall into the class $P = 1$ of icosadeltahedra as was predicted by Caspar and Klug (1962). The data support their hypothesis that families of icosahedra would be developed by altering the distance between the points of insertion of the five-fold axis. This capsid protein defect also results in the incorporation of much of the capsid protein, into large cytoplasmic aggregates of protein and RNA. These observations support models suggesting that the geometry of a pre-formed nucleocapsid organizes the assembly of the virus membrane proteins into a structure of identical configuration and argues against models suggesting that assembly of the membrane glycoproteins directs the assembly of the nucleocapsid.

© 2003 Elsevier Science (USA). All rights reserved.

Introduction

Sindbis virus is the prototype of the alphavirus genus in the *Togaviridae* family of viruses. The family includes many significant human and animal pathogens, such as Western Equine Encephalitis Virus (WEEV), Eastern Equine Encephalitis Virus (EEEV), Ross River Virus (RRV), and Venezuelan Equine Encephalitis Virus (VEEV).

Sindbis virus is composed of a protein/RNA nucleocapsid surrounded by a membrane envelope, which contains two glycoproteins (E1 and E2) (Brown et al., 1972; Harrison, 1986; Strauss and Strauss, 1994). The nucleocapsid is constructed with a single molecule of viral genomic RNA of 11703 nucleotides and 240 copies of the capsid protein (C;

30kD) and has icosahedral $T = 4$ symmetry (Coombs and Brown, 1987a; Paredes et al., 1993; Paredes et al., 1992). In the mature virus particle the nucleocapsid is enveloped by a membrane containing 80 heterotrimers of E1 (58kD)-E2 (53kD) which form a $T = 4$ icosahedral lattice complementary to the structure of the nucleocapsid itself (Coombs and Brown, 1987a; Paredes et al., 1993). The E1 and E2 proteins span the membrane bilayer and E2 specifically binds to the nucleocapsid protein through contact with its 33 amino acid endodomain (Lee and Brown, 1994; Lee et al., 1996; Lopez et al., 1994). The structure of the mature virion is, therefore, architecturally complex. The virion consists of two geometrically identical icosahedral shells nested one within the other. A membrane bilayer is sandwiched between the two protein shells. The two shells are joined to one another by protein-protein interactions between E2 of the outer shell and the capsid protein of the inner shell. The outer shell is stabilized by molecular interactions among its E1 glycoproteins. We have shown that intramolecular disulfide bridges in the E1 glycoproteins (Anthony and Brown, 1991; Carleton and Brown, 1996; Mulvey and Brown, 1994) sta-

* Corresponding author. Fax: +1-919-515-2047.

E-mail address: dennis_brown@ncsu.edu (D.T. Brown).

¹ Present address: Universidade Federal do Rio de Janeiro, CCS, Bloco I, Departamento de Virologia, Ilha do Fundão, Rio de Janeiro, RJ, 21941-590.

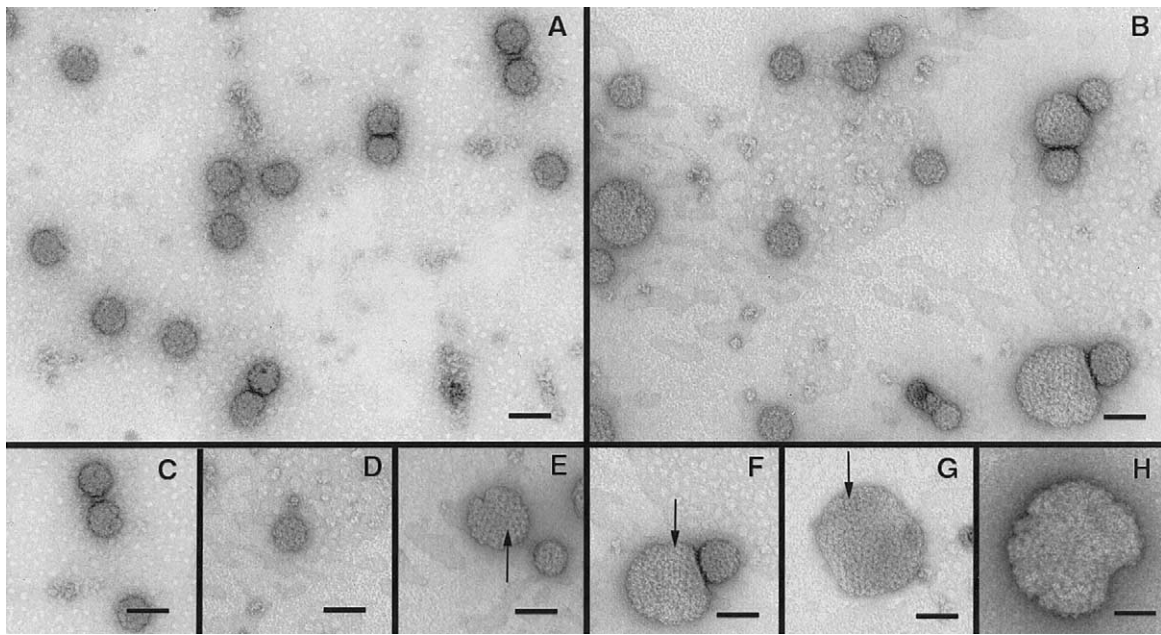


Fig. 1. Electron micrographs of negatively stained virus particles recovered from the supernatant of BHK cells transfected with either Sindbis virus S420Y (A, C) or Y180S/E183G (B, D, E, F, G, H). A and B, a wider view of the fields. C–H, Individual particles arranged to show examples of the various sizes found for the Y180S/E183G mutant (D–H) as compared to the control S420Y particle (C). Arrows point to morphological units. Bars, 100 nm.

bilize a scaffold of E1-E1 interactions that are responsible for the icosahedral structure of the virus surface (Anthony and Brown, 1991; Anthony et al., 1992; Pletnev et al., 2001).

The structural proteins are encoded as a polyprotein (130 kDa), in the order $\text{NH}_2\text{-C-pE2(E3-E2)-6K-E1-COOH}$ (Strauss and Strauss, 1994). The capsid protein is cleaved by autoproteolysis from the polyprotein, exposing the N-terminal signal sequence which is translocated into the membrane of the Endoplasmic Reticulum (ER) (Bonatti et al., 1984; Lilijestrom and Garoff, 1991; Wirth et al., 1979). This polyprotein (100 kDa) is further cleaved in the lumen of the ER by the cellular enzyme signal peptidase and is modified by glycosylation and fatty acid acylation. In the ER, heterotrimers of E1 and pE2 are formed and the trimers are exported to the Golgi Complex (GC) and finally to the plasma membrane (Carleton and Brown, 1996). During movement through this pathway, E3 is cleaved from pE2 and is lost to the medium.

The assembly of the alphaviruses occurs through independent but converging pathways. While the envelope spikes are assembled and exported through the secretory pathway the cytoplasmic capsid proteins associate with the 49S genomic RNA to form the $T = 4$ icosahedral nucleocapsid (Coombs and Brown, 1987a; Coombs and Brown, 1987b; Paredes et al., 1993; Paredes et al., 1992; Tellinghuisen et al., 2001). The assembled nucleocapsid joins the trimers of envelope glycoproteins at the plasma membrane through a specific interaction between the endodomain of E2 and a hydrophobic cleft in the capsid protein (Lee and Brown, 1994; Lee et al., 1996; Lopez et al., 1994). During the budding process 240 repeated interactions of this type help drive the assembly of the virus membrane and align the

E1-E2 trimers into trimer-trimer associations, which reflect the geometry of the nucleocapsid.

To identify the domain of the capsid protein which bound the E2 tail Lee and Brown (1994) produced mutations in the capsid protein that altered the association of E2 with the capsid (Lee and Brown, 1994). This mutant has amino acid substitutions in a domain of the capsid protein that had been previously shown to be exposed on the surface of the intact nucleocapsid (Coombs and Brown, 1987b). This mutant, Y180S/E183G, produced virus with reduced infectivity compared to wild type (Lee and Brown, 1994). X-ray crystallography revealed a structural rearrangement in the hydrophobic cleft of the mutant capsid protein in which a tryptophan at position 247 had moved into the cleft occupying an area vacated by the loss of Y180 density (Choi et al., 1996). This mutant had functional envelope glycoproteins (Lee and Brown, 1994). The mutation in the capsid was also found to result in some of the progeny virus having a larger than normal diameter. In the research presented below we describe a further analysis of this mutant's phenotype in infected cells and we have, particularly, focused upon the effect of these mutations in the capsid protein on the process of virus assembly.

The data presented support a model that alphavirus budding is driven by the one- to-one binding of spike protomers to capsid proteins in the pre-assembled nucleocapsid and that such a process causes the spikes in the viral envelope to organize into a geometrical arrangement which reflects the geometric organization of the nucleocapsid (Anthony and Brown, 1991; Brown, 1980; Cheng et al., 1995; Garoff and Simons, 1974; Harrison, 1986; Lee et al., 1996; Pletnev et al., 2001). This model has been challenged by a model in

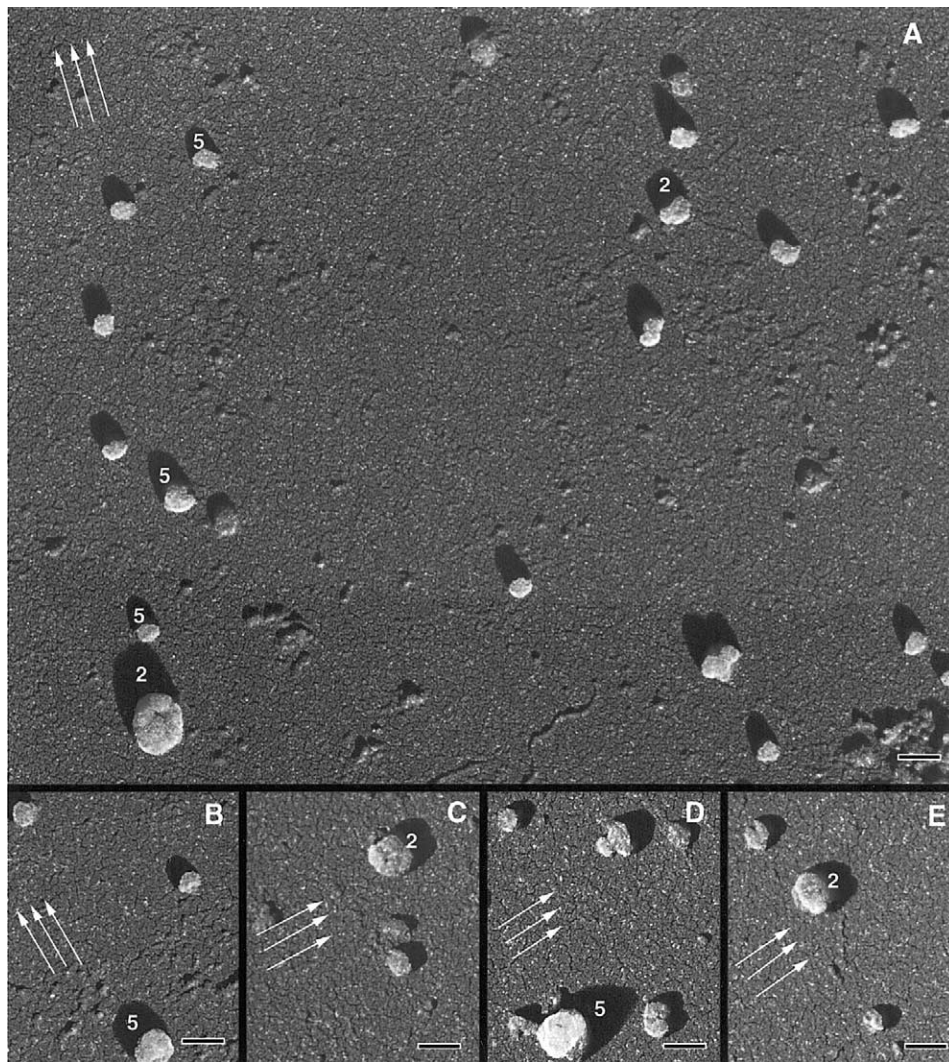


Fig. 2. Electron micrographs of particles recovered from supernatants of BHK cells transfected with the Y180S/E183G mutant prepared by Critical Point Drying. The supernatant of transfected cells was added to a 15–35% equilibrium potassium tartrate gradient and the virus band processed as described in Materials and Methods. The shadows produced show the square shape typical of the shadow of an edge (2-fold Axis) and the pointed shape typical of the shadow across a vertex (5-fold axis) of an icosahedron (2 and 5, respectively). The triple arrows show the direction of the shadowing; Bars, 100 nm.

which assembly of the membrane proteins organizes the icosahedral conformation of the alphavirus nucleocapsid (Forsell et al., 2000). In the research presented herein we show that a mutation in the capsid protein produces virus particles in which the wild type membrane glycoproteins are assembled into icosahedra of different triangulation numbers, suggesting that the conformation of the capsid protein determines the assembly of the virus envelope.

Results

Electron microscopy of Y180S/E183G virus particles

Caspar and Klug (1962) were inspired by the architectural principles applied in the construction of geodesic domes and the resemblance of these structures to the protein

shells of icosahedral viruses. They recognized that the assembly of space-enclosing structures such as virus capsids could only be accomplished with genetic efficiency if the structures were constructed of multiple copies of identical morphological subunits. They concluded that there could be only one way in which iso-dimensional shells could be constructed from a large number of identical protein subunits, and that such assembly would lead to icosahedral symmetry in the mature virion. Most importantly, they stated that virus subunits organized on this scheme would have the property of self-assembly into a shell of definite size. Some degree of deformation would be tolerated in the packing of the protein subunits in order to accommodate interactions at a different axis of symmetry in the icosahedral structure, a principle that they named “Quasi Equivalence.” Caspar and Klug also demonstrated that a single type of morphological subunit could be assembled into

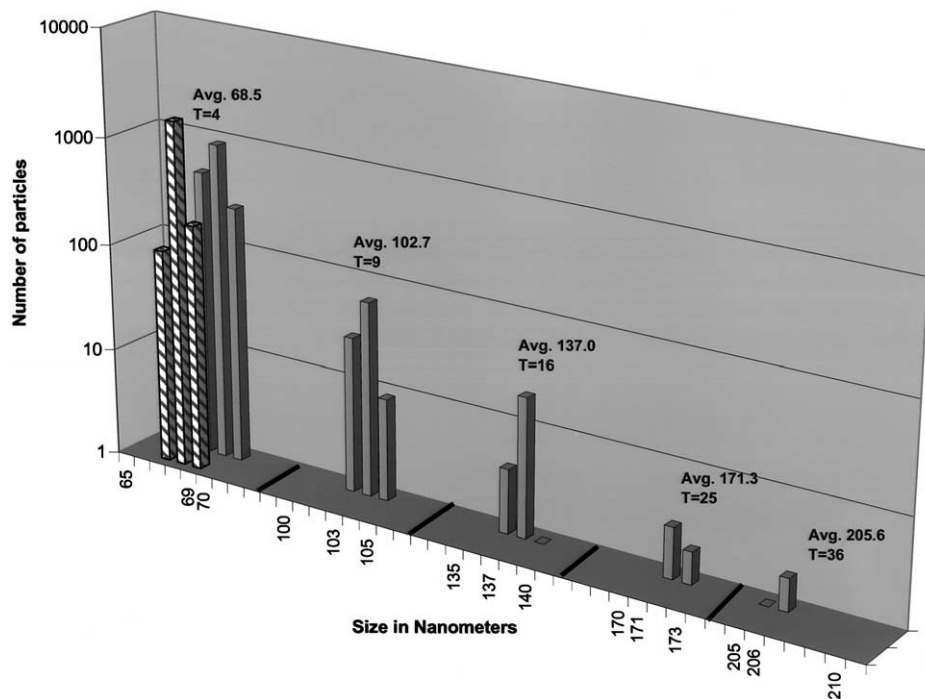


Fig. 3. Size distribution of particles produced by infection with the Y180S/E183G mutant (solid) or wild type virus (hatched). The particles were concentrated by equilibrium density gradient centrifugation (Methods) and the virus band was examined by electron microscopy after Critical Point Drying. The mutant virus particles were distributed into 5 distinct size classes and particles having diameters between these classes were not found (Avg. is the average of the particles clustered in that region of the distribution). The various size classes were assigned triangulation numbers (T) based on the measured diameter as described in the text. The data for the mutant represents a total of 1813 particles measured.

icosahedra having different sizes by altering the distance between the points of insertion of the five-fold axis. That this can happen in nature has been demonstrated in the bacterial viruses where morphological variants having different triangulation numbers have been identified (Walker and Anderson, 1970).

To our knowledge, mutations leading to the assembly of morphological variants with altered triangulation numbers in animal viruses have not been produced. Some animal viruses seem to produce a limited number of such variants spontaneously and mutations have been produced which result in the production of multi-cored particles (Gaedigk-Nitschko and Schlesinger, 1991; Skoging-Nyberg and Liljestrom, 2001; Strauss, 1978). We have previously shown that the Sindbis virus capsid mutation Y180S/E183G produces mature particles with size and shape indicating icosahedral symmetry but which are larger than normal (wild type) particles (Lee and Brown, 1994). We have conducted experiments to further characterize the structure and assembly of these particles.

When BHK cells are either transfected or infected (as described in Methods) with the Sindbis virus capsid Y180S/E183G mutant, virus particles of several different sizes are recovered in the media. Fig. 1 shows electron micrographs of negatively stained preparations of such particles, which are found in a range of sizes. The wild type size is the predominating species (Fig. 1 and 3) and the larger sizes

represent progressively smaller percentages of the total suggesting that the assembly of larger particles is more difficult or otherwise infrequent. The particles all possess distinct subunit structure and in many cases subunits are seen organized in morphological units (Fig. 1), as is the case in the wild type virus (Paredes et al., 1993; Von Bonsdorff and Harrison, 1978).

Structural analysis of particulate material by conventional negative staining results in the production of images of particles which are deformed by the drying process (see Fig. 1). While this procedure produces very detailed information on the substructure of the particle, conclusions regarding the true size and shape are not as reliable and become even less reliable as the particles become larger and less geometrically strong. The best way to establish the three dimensional conformation of these larger particles is by electron-cryo microscopy which we have successfully used to examine the surface and core structure of Sindbis virus (Paredes et al., 1993; Pletnev et al., 2001). Unfortunately the numbers of large particles produced in a preparation is so small that, to date, it has not been possible to generate sufficient numbers of particles to allow a reconstruction. To overcome this problem and to overcome the drying artifacts associated with conventional negative staining, we prepared the particles by the technique of "Critical Point Drying" which preserves three-dimensional structure (Anderson, 1954). Images of particles prepared by this pro-

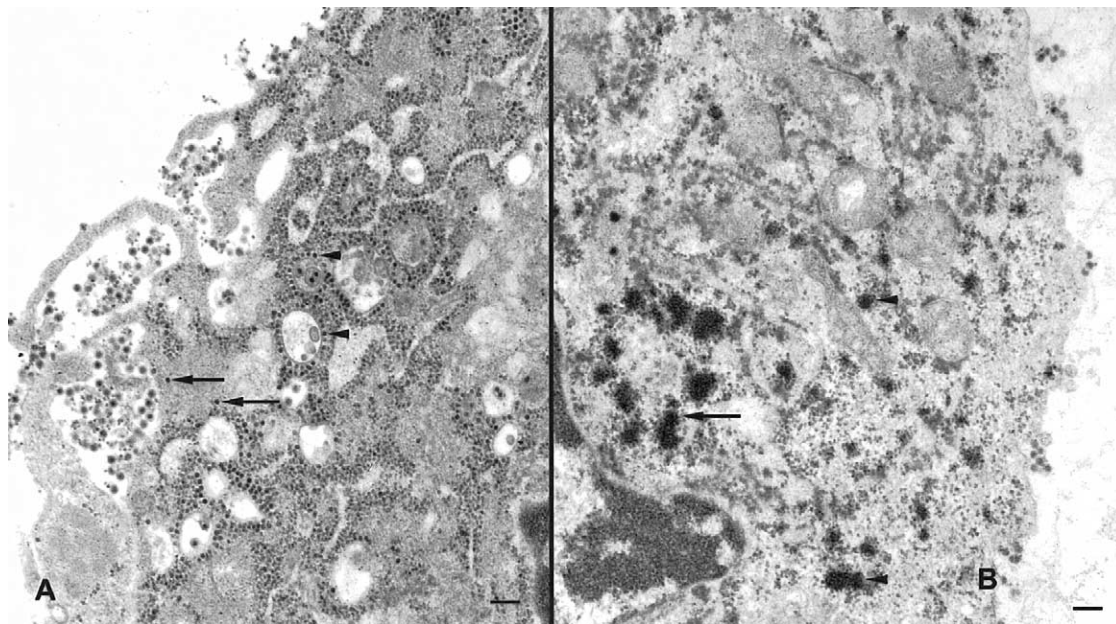


Fig. 4. Electron micrographs of ultra thin sections of BHK cells transfected with S420Y (A) or Y180S/E183G (B). In A, typical infection of Sindbis virus in these cells, showing capsids free in the cytoplasm (arrows) and attached to membranes (arrow heads). Mature virus particles are seen outside the cell. In B, electron dense inclusions are observed either around an apparent CPV-1 (arrow: see text) or scattered in the cell cytoplasm (arrow head). Bars, 200 nm.

cedure are shown in Fig. 2. Contrast is produced, in this procedure, by the deposition of heavy metal (platinum) onto the specimen, by evaporation, from an angle of about 40 degrees. The deposited metal obscures the subunit structure and the angular appearance of the virions. The very sharp and well defined nature of the shadows produced by the particles, however, allows an accurate measure of the cross sectional diameter (Coombs and Brown, 1987b). The shadows produced do, in some instances, show the pointed shape typical of the shadow across a vertex (5-fold axis) and the square shape of the shadow of an edge (2-fold axis) that would be expected of an icosahedron (Coombs and Brown, 1987b; Williams and Smith, 1958) (Fig. 2). The critical point dried particles were found to be distributed into 4 discrete and easily distinguished size classes (Fig. 3). The average diameter of the classes were 68.5 nm, 102.7 nm, 137.0 nm, and 171.3 nm. We were unable to find the largest particle seen in the negatively stained preparations in the critical point dried preparations; however, measurements obtained from negatively stained virions indicate that this largest variant would be approximately 205 nm in diameter. The larger diameter particles were not found in preparations of wild type virus (Fig. 3).

The equations presented by Caspar and Klug (1962) and used by Brown and Gliedman (1973) can be used to predict the triangulation numbers of the morphological variants produced by the Y180S/E183G mutant. According to Caspar and Klug (1962), any icosadeltahedron has $20T$ subtriangles where T is the triangulation number given by the rule: $T = Pf^2$ where P can be any number of the series 1, 3, 7, 13, 19, 21, 31, 37... ($P = h^2 + hk + k^2$, for all pairs of integers h and k having no common factor) and f is any

integer. The value of f increases from 1 upward for a fixed value of P , and corresponds to successive subtriangulations of the primitive deltahedron. The equation $T^{1/2} = 0.618D/d$ will give the triangulation number for any icosahedron where T is the Triangulation number, D is the Diameter of the particle and d is the center to center spacing of the basic structural unit (capsomere). For wild type Sindbis virus the diameter of the particle is found to be 68.5 nm and the distance between the capsomeres (d) is 21.16 nm.

We used the average particle diameters (D) presented in Fig. 3 to predict triangulation numbers and these predicted values are also shown in Fig. 3. Using the equation presented above we obtained triangulation numbers: $T = 4$, $T = 9$, $T = 16$, $T = 25$ and $T = 36$ (Fig. 3). These values match the predictions for a series of commonly constructed icosahedra in the $P = 1$ symmetry group (Caspar and Klug, 1962).

Fig. 3 also shows the relative amounts of the variants produced by the capsid mutation and summarizes the results of nearly 2000 measurements of particle diameter. The wild type size particle accounts for approximately 90% of the total virus produced. Less than one virus in 10 has the $T = 9$ morphology, about one particle in 100 has the $T = 16$ structure and about one particle in 500 has the $T = 25$ structure.

Morphogenesis of Y180S/E183G mutants in BHK cells

The data presented above suggest that the mutations in the capsid protein appear to have affected the capacity of the capsid protein to be assembled into only one, $T = 4$, icosahedral configuration. We examined thin sections of

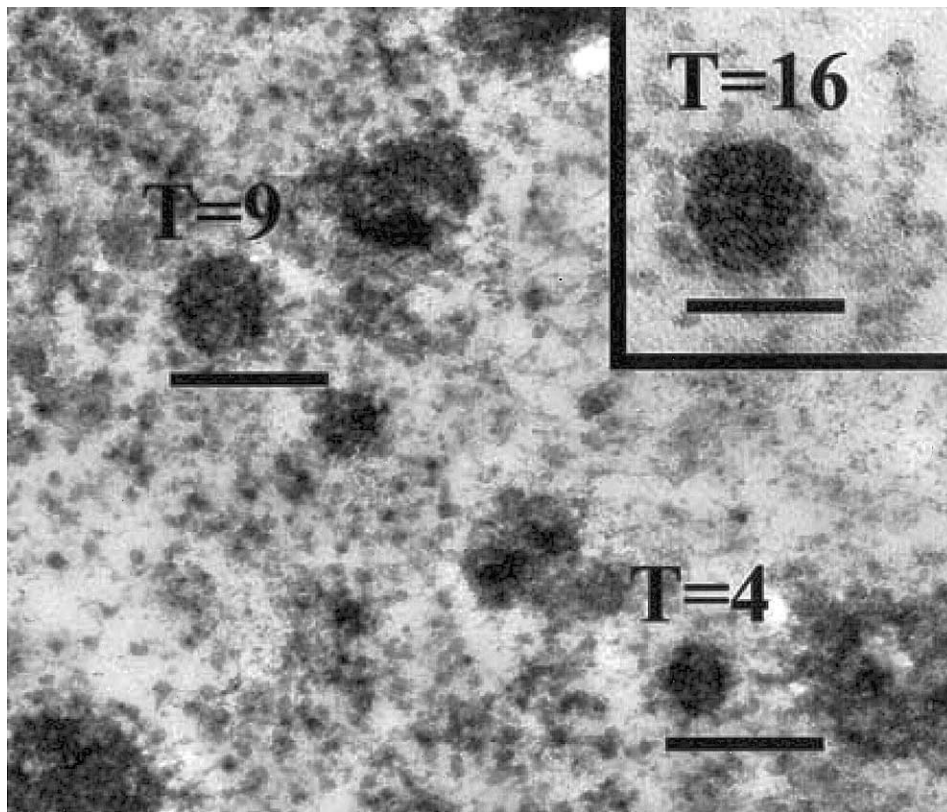


Fig. 5. Electron micrographs of nucleocapsids in the cytoplasm of Y180S/E183G infected cells. Cores are identified which correspond to predicted triangulation numbers of $T = 4$, $T = 9$ and $T = 16$. Bars, 100 nm.

mutant and wild type infected cells by electron and light microscopy to determine if the intracellular pattern of virus morphogenesis was also affected. In the electron microscope, wild type infected cells show a typical pattern of virus nucleocapsids free in the cytoplasm and attached to cellular membranes (Fig. 4A). Many mature virions are also seen outside the infected cell. By contrast the mutant infected cells show fewer mature virions at the cell surface and nucleocapsids are not as readily detected in the cell cytoplasm (Fig. 4B). Attempts to find assembled nucleocapsids reflecting the various sizes implied by the analysis of the mature virions was very difficult. This was due in large part to the relative insensitivity of thin section electron microscopy to detect structures present in low copy number. This problem was compounded by the fact that the larger structures represent a minority of the virus cores produced. Images of the cell cytoplasm are also confused by the presence of amorphous aggregates (see below). While all of these problems combined to make the task difficult we were able to identify structures, in thin sections of mutant virus infected cells, which appeared to contain cores of normal $T = 4$ (39.0 nm diameter), variant $T = 9$ (58.4 nm diameter) and variant $T = 16$ (78.0 nm diameter) size classes (Fig. 5).

The cytoplasm of the mutant infected cells shows the presence of electron-dense inclusions that are not seen in

cells that are infected with the wild type virus (Fig. 4). The electron dense inclusions are dispersed in the cell cytoplasm and frequently are seen organized around an internal structure much as capsids are seen organized around an internal vesicle in wild type infected cells (Fig. 4A). The inclusions are so large and appear with such frequency in the mutant infected cells that they can be easily seen at the light microscope level as very large and dense bodies in the cell cytoplasm (Fig. 6). The inclusions are very electron-dense aggregates, which at high magnification have a distinct granular appearance (Fig. 7). Their staining properties (similar to that of chromatin) suggest that they contain nucleic acid and protein. As the mutation resulting in the production of these aggregates resides in the capsid protein, it is reasonable to expect that these aggregates contain capsid protein. Positive determination that the dense bodies contain capsid protein by immunocytochemical localization was not possible as we have found that it is a property of the capsid protein that it binds strongly, although nonspecifically, to IgG molecules (Miller and Brown, 1993). That these inclusions contained protein, likely virus capsid protein, was further suggested in experiments in which Y180S/E183G transfected cells were processed for electron microscopy and the resulting thin sections were treated with Proteinase K as described in Methods. Treatment with protease pro-

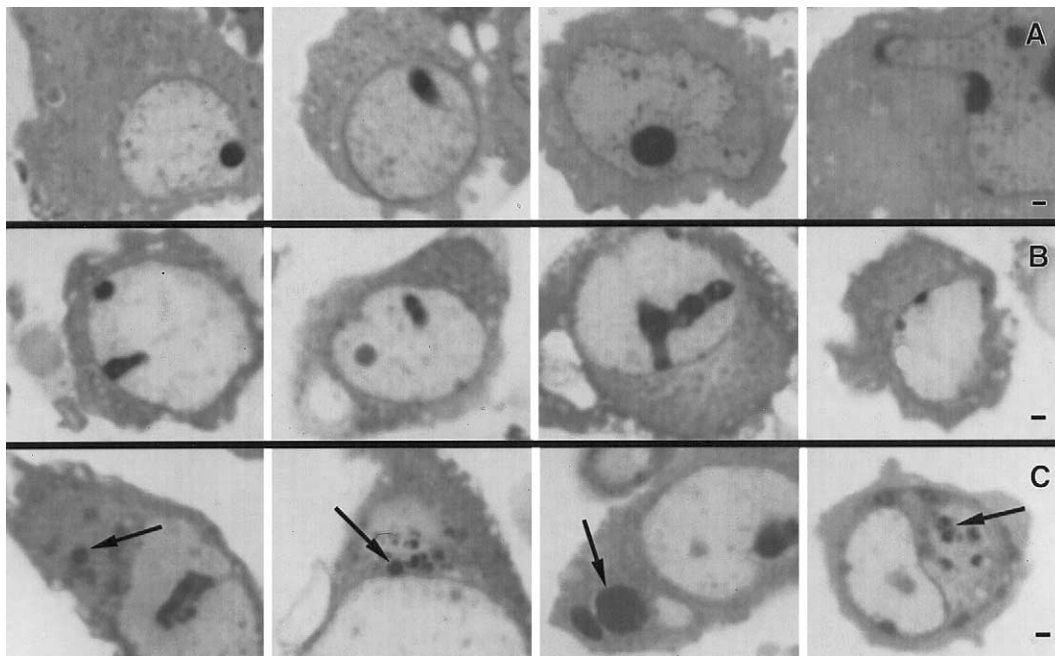


Fig. 6. Light microscopy of uninfected BHK cells (A); BHK cells transfected with S420Y Sindbis virus (B) or transfected with the Y180S/E183G Sindbis virus mutant (C). The images are from thick sections of the same material prepared for electron microscopy (Fig. 4) as described in Materials and Methods. Note the large, dense bodies (arrows) that are observed in the cytoplasm of the Y180S/E183G transfected cells. Bars, 20 μ m.

duced images of the mutant infected cells in which the electron dense inclusions were lost leaving holes in the sections (Fig. 8). These data suggest that the dense bodies contain protein and possibly RNA packed so tightly that the embedding compound only poorly penetrates the structure.

The majority of these inclusions are found around vacuoles that are very similar to the CPV-1 reported by Friedman and which are seen in wild type infected cells (Friedman et al., 1972; Grimley et al., 1968) (Figs. 4, 7, 8C). These data further suggest that these inclusions are composed of mutant capsid protein. The protein seems to accumulate around vacuoles that may be of lysosomal origin (Froshauer et al., 1988) where it has been suggested virus RNA synthesis takes place (Froshauer et al., 1988; Luo and Brown, 1994). The data suggest the possibility that a large amount of mutant virus protein assumes a conformation capable of binding virus RNA but incapable of forming icosahedral shells.

Infectivity of the morphological variants

It was of interest to know whether the larger particles, produced by the mutant virus, were infectious. Sindbis virus S420Y or the Y180S/E183G mutant was grown in BHK cells in the presence of met/cyst 35 S (as described in Methods). Virus supernatant was centrifuged through a two-step K-tartrate gradient (described in Methods). The resulting virus band was collected and centrifuged through a continuous, 15% to 22%, sucrose gradient from which peaks of

radioactivity were analyzed. The mutant virus gradient profile shows that radioactivity accumulates in several peaks not seen in the wild type profile (Fig. 9). The different peaks were tested for their ability to form plaques on BHK cells and the titers compared to the cpm values obtained in the same fraction to create a value for specific infectivity in terms of PFU/CPM (Fig. 9, table). We found that most of the peaks found for the double mutant are associated with some infectivity. We have previously shown that virus produced by this mutant at 28°C are 5% as infectious as wild type virus (Lee and Brown, 1994). We suggested that the reduced infectivity may reflect the presence of the larger particles. In these experiments we find that the large particles account for about 10% of the total virus produced at 28°C (Fig. 3). When the ratio of infectivity to CPM is determined for each of the fractions produced by the mutant it is found that the peaks putatively containing the larger particles have a maximum of about 3% the infectivity of the putative normal size virions (Fig. 9, fractions 20 and 22). These results suggest that the larger particles have very low infectivity if the infectivity in those peaks is not due to contamination with normal size particles. Although large virus particles could be seen in these fractions the concentration of virus in these peaks was too low to resolve this latter point by electron microscopy. Since our previous work (Lee and Brown, 1994) showed that the entire virus population produced (normal and large size particles) have only 5% the infectivity of wild type virus, we conclude that the normal size particles ($T = 4$) also have a very high particle to infectious unit ratio.

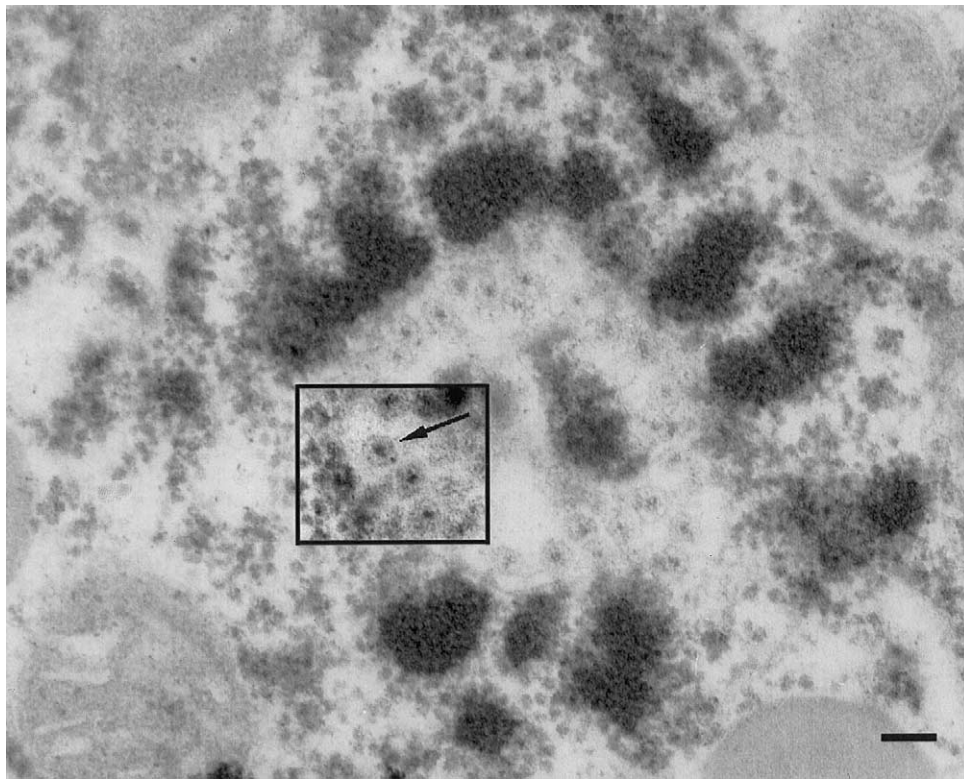


Fig. 7. Higher magnification electron micrograph of an inclusion around a CPV-1 vacuole observed in the cytoplasm of Y180S/E183G transfected BHK cells. The insert uses contrast enhancement to show the CPV structure (arrow). Bar, 100 nm.

Discussion

The data presented above show that a mutation in the Sindbis virus capsid protein (Y180S/E183G) produces morphological variants that fall into distinct size classes. These morphological variants fall into the possible triangulation numbers described by Caspar and Klug (1962). According to Caspar and Klug, the self-assembly of any icosahedral virus will result in a structure having a pre-determined triangulation number. This process of self-assembly occurs as protein subunits and nucleic acid interact at their lowest energy state (Caspar and Klug, 1962). The data presented here suggest that the mutations Y180S/E183G result in a distortion or freedom of movement in the capsid protein which permit C protein-protein interactions which allow the formation of protein shells of increasing triangulation numbers. Structural analysis of the mutant capsid protein by X-ray crystallography revealed a conformational change in the hydrophobic domain responsible for attachment of the capsid protein to the E2 endodomain (Choi et al., 1996). While this mutation is likely away from the domains of capsid protein-protein interactions, it appears that this change also allows for the formation of the variant nucleocapsids by affecting these areas of contact during assembly. Although the negatively stained material suggested that the particles were organized in morphological units (Fig. 1, arrows) and were true icosahedra, confirmation came through two observations: first, large particles observed

after preparation by the critical point drying technique, where the 3D-morphology is preserved, show 2- and 5-fold axis of symmetry (Fig. 2); and second, the triangulation numbers predicted for the different size particles, based on their measured diameters, fall into the possible categories of triangulation numbers according to Caspar and Klug and do not produce nonpredicted values. The fact that the variants formed by the mutant fall into a predicted series of triangulation numbers, the $P = 1$ series, suggests that mutant capsid protein in a particular configuration only interacts with other protein having an identical configuration. Alternatively capsid protein in a particular configuration may serve as a scaffold to reorganize or fold other capsid protein into an identical configuration. The observation that the variants produced by the mutant Y180S/E183G fall into the $P = 1$ series of Icosahedra ($T = 1, 4, 9, 16, 25, 36$) and do not include members of other classes ($T = 7, 13$ etc) supports a prediction made in the original hypothesis of Caspar and Klug (1962). Caspar and Klug proposed that the most efficient way to produce families of icosahedra was to simply extend the number of sub triangles incorporated into the two-fold axis. This would allow the morphological units to interact with one another in the same way in all size classes. Incorporating the subunits into other P classes would require subunit interactions which are different and would be less energetically favored. We found that the normal sized particle is most frequently assembled (90% of the total particles produced), and frequency decreases as the

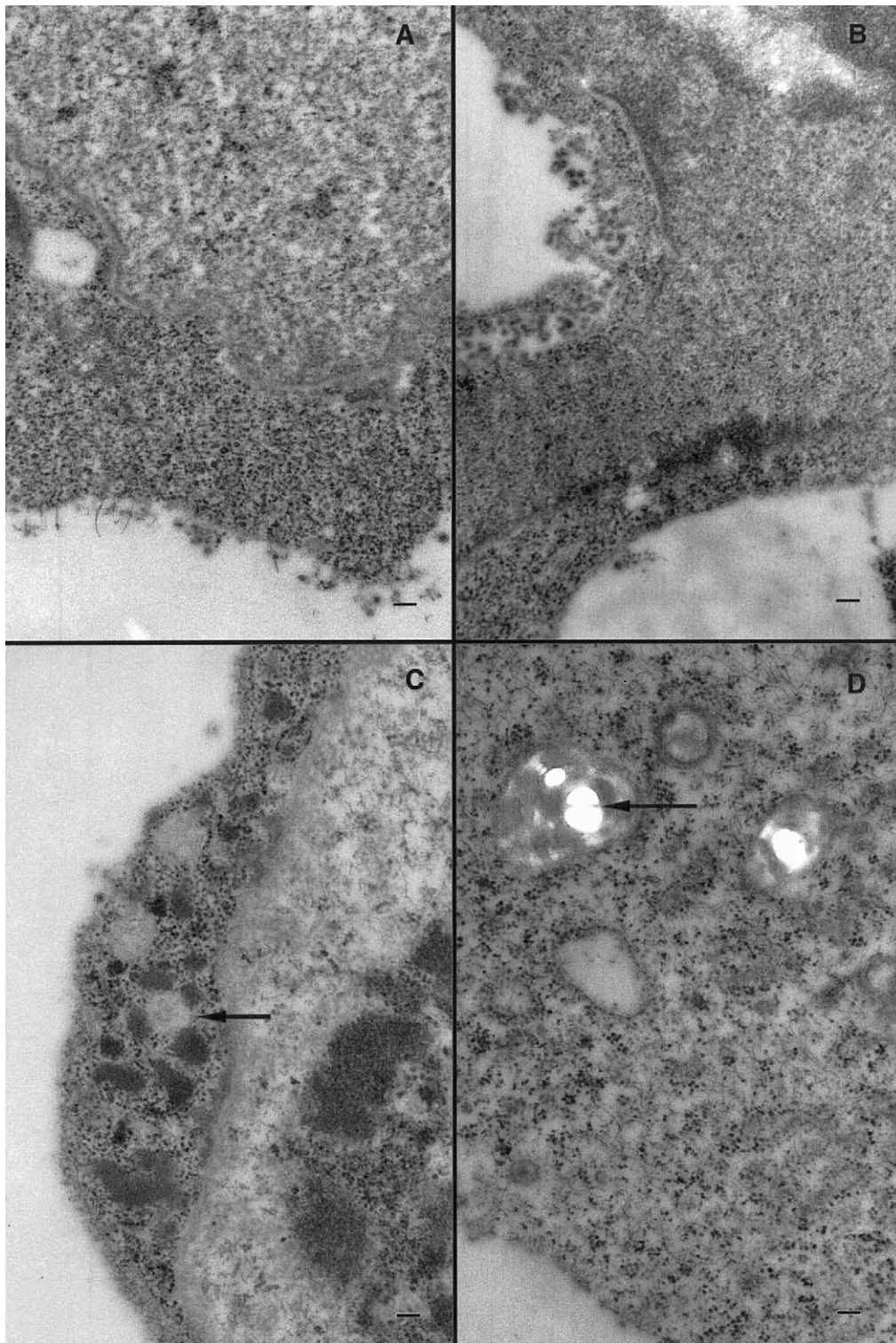
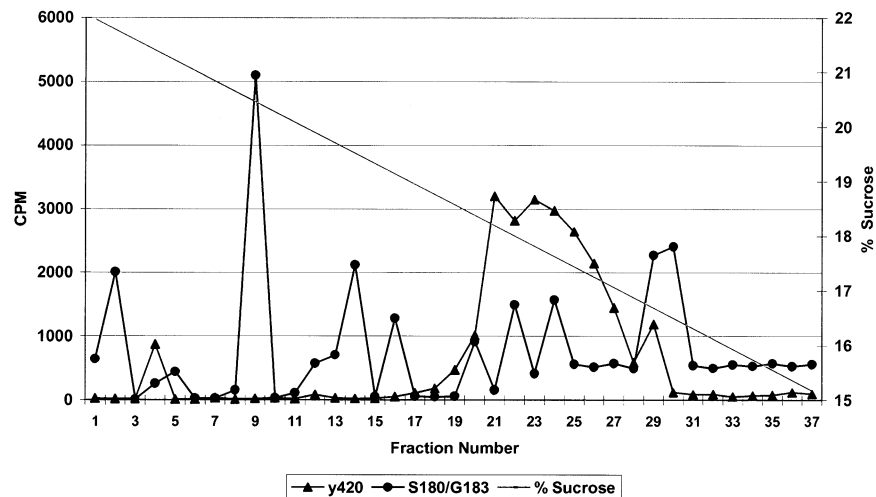


Fig. 8. Electron micrographs of BHK cells transfected with either S420Y (A, B) or Y180S/E183G (C, D) Sindbis virus and treated (B, D) or not treated (A, C) with proteinase K (2 ng/ μ L). Note the electron dense inclusions in C (arrow) that appear to be replaced by holes in D (arrow). Bars, 200 nm.

particle size increases (Fig. 3). Apparently the $T = 4$ configuration (68.5 nm) is preferred over the other triangulation numbers even for the mutant. This observation is in agreement with a recently published observation by Zhang et al. (2002).

The cytoplasm of cells transfected with the mutant virus show inclusions that are so large they can be seen by light microscopy (Figs. 4, 6, and 7). These inclusions are found primarily around CPV-1-like vesicles, but are also found in small patches in the cytoplasm. The fact that these CPV-1



Specific Infectivity of Y180S/E183G

Fraction	2	4	5	9	13	14	16	20	22	24	30
Titer (pfu/ml)	1.1×10^4	5.0×10^4	2.0×10^4	6.0×10^4	1.0×10^5	4.0×10^5	8.5×10^5	2.0×10^6	1.0×10^7	1.5×10^6	4.5×10^6
Infectivity	0.3	9.6	2.2	5.9	7.0	9.5	33.3	109.3	334.0	47.7	93.5

Fig. 9. The Specific infectivity ratio of virus morphological variants. Virus supernatants from BHK cells transfected with either S420Y or Y180S/E183G were centrifuged through a two step K-tartrate gradient (described in Methods) and the resulting virus band was collected and centrifuged through a continuous, 15% to 22%, sucrose gradient. The peaks of radioactivity produced by this velocity sedimentation were analyzed as described in Methods. The table presents values for the Y180S/E183G peaks in PFU and PFU/CPM.

structures are centers for virus RNA replication and nucleocapsid formation (Friedman et al., 1972; Froshauer et al., 1988) strongly suggests that the electron dense bodies observed are in fact mutant capsid protein and RNA aggregates. Furthermore, proteinase K treatment completely removes the inclusions, confirming the protein content of these bodies. The large amount of protein accumulating in deposits in the cytoplasm of the mutant infected cells suggests that much of the protein assumes conformations which do not lead to assembly into icosahedra.

The inclusions around CPV-1-like vesicles were more frequent when the cells were incubated at 28°C instead of 37°C. At 28°C we also obtained the largest amount of the larger particles (Lee and Brown, 1994). These data suggest that lower temperatures favor the interactions between the capsid proteins that lead to the formation of the inclusions and the larger particles.

The wild type Sindbis virus has a $T = 4$ geometry. The data presented above show that a mutation in the capsid protein can result in the assembly of virus in icosahedra of different triangulation numbers. The membrane glycoproteins in the mutant are wild type in sequence (Lee and Brown, 1994; Lee et al., 1994), and thus it appears that the formation of variants is the product of the mutation in the capsid protein. Assembled nucleocapsids corresponding in size to those predicted for some of the morphological variants could be found in cell cytoplasm. These observations support models suggesting that the geometry of a pre-formed nucleocapsid organizes the assembly of the virus

membrane proteins into a structure of identical configuration (Brown, 1980) and argue against the model suggesting that assembly of the membrane proteins directs the assembly of the nucleocapsid (Forsell et al., 2000). This conclusion is supported by previous observations showing: 1) The formation of nucleocapsids in mutants having defects in the membrane proteins which prevent capsids from attaching to membranes (Brown and Smith, 1975). 2) The formation of capsids in cells treated with drugs which block the exposure of the E2 endo domain to the cytoplasm preventing the association of the capsid with the membrane (Liu and Brown, 1993a). 3) The formation of tubular and multi-cored particles (Gliedman et al., 1975; Strauss et al., 1977). 4) The in vitro assembly of capsids by purified capsid protein and nucleic acid (Tellinghuisen et al., 1999; Tellinghuisen and Kuhn, 2000).

Materials and methods

Cells, virus and media

Baby hamster kidney cells strain 21 (BHK-21) used in this study were initially provided by Peter Faulkner (Queens University, Kingston, Ontario, Canada). These cells were maintained in Eagle Minimum Essential Medium (MEM) supplemented with 10% Fetal Bovine Serum (FBS), 5% tryptose phosphate broth (TPB), 2mM glutamine and 50 µg/ml gentamicin as described previously (Condreay and

Brown, 1988). The wild-type Sindbis virus was produced from the Toto 1101 cDNA clone of Sindbis virus containing a tyrosine at E2 position 420, S420Y. This clone has been described by Liu and Brown and has been shown that this change has no effect on virus replication or assembly and serves as the wild-type construct for the mutagenesis, *in vitro* transcription, and transfection experiments (Liu and Brown, 1993b).

In vitro transcription and RNA transfection

Full-length mutant or wild-type cDNA was first linearized by *Xho*I, treated with proteinase K, phenol extracted, and ethanol precipitated. Templates were then used for *in vitro* runoff transcription with SP6 RNA polymerase as described previously (Liu and Brown, 1993b; Rice et al., 1987). About 1 μ g of linearized wild-type or mutant Sindbis virus cDNA was mixed with 1 mM each of ATP, UTP and CTP; 0.5mM of GTP; 1 mM of m⁷GpppG; 10 units of RNase inhibitor and 40 units of SP6 RNA polymerase in 20 μ l of 1 \times SP6 RNA polymerase buffer (40 mM Tris-HCl pH 7.9, 6 mM MgCl₂, 2 mM spermidine, 10 mM DTT). The mixture was incubated at 40°C for 1 h. Two microliters of the reaction was checked on 1% agarose gel for quality and yield. Templates were removed using 20 units of RNase free DNase 1. The RNA transcripts were introduced into BHK-21 cells by electroporation as described by Liljeström and Garoff (1991). Ninety percent confluent BHK-21 cell monolayers were used for the transfection. Cell monolayers were trypsinized, cells were pelleted and washed once with RNase-free electroporation buffer PBS-D (2.7 mM KCl, 1.5 mM KH₂PO₄, 137 mM NaCl, and 8 mM Na₂HPO₄) in diethyl pyrocarbonate (DEPC)-treated water. Washed cells were resuspended in PBS-D to a concentration of 1.2×10^7 cells/ml. Twenty microliters of RNA transcripts and 400 μ l of cell suspension were mixed and transferred to a 0.2-cm gap length cuvette. Electroporation was performed under the following conditions: 1.5k V, 25 μ F, and ∞ resistance. Cells were pulsed once. Healthy cells give a time constant of 0.7 under these conditions. After the pulse, cells were allowed to sit for 10 min before transfer into 10ml of MEM medium. Cells and supernatants were harvested at 16 h post transfection.

Titration of virus production (plaque assay)

Titration of Y180S/E183G double mutant viruses and S420Y virus grown in BHK-21 cells was done on BHK-21 cells. All virus stocks were kept frozen at -80°C in MEM medium as described above, with the addition of 10% glycerol and were never thawed until the dilutions were made. For plaque assay on BHK-21 cells, 1×10^7 to 2×10^7 BHK-21 cells are plated onto one 25-cm² flask in growth medium at least 12 h before infection. Virus dilutions were prepared in PBS-D with 3% FBS and held in ice baths through the plaque assay. Two hundred microliters of each

virus dilution was placed onto the cell monolayers and viruses were allowed to adsorb for 1 hr at room temperature. After the adsorption, cell monolayers were overlaid with 1% agarose in 1 \times MEM. The plaques were incubated at 37°C for 2 days before staining with 2% neutral red in 1% Agarose and 1 \times PBS-D.

Production of labeled virus

Subconfluent monolayers of BHK-21 cells in 75-cm² flasks were treated with 4 μ g/ml Actinomycin-D (from Calbiochem-Novabiochem Co. La Jolla, CA) for 90 minutes. The cells were then infected with either S420Y or Y180S/E183G virus (multiplicity of infection, m.o.i. = 1) and incubated for 3 h and 45 min at 37°C (S420Y) or 28°C (Y180S/E183G). Monolayers were washed twice with PBS and starved in methionine and cysteine free medium containing 1% FBS, 5% TPB, 2 mM glutamine and 10 mM HEPES. After one h incubation at 28°C or 37°C, the medium was replaced by the above starvation medium containing 50 μ Ci/ml [³⁵S]Met/Cys protein labeling mix (NEN Life Science Products Inc., Boston, MA). The monolayers were incubated at 28°C or 37°C until harvest of supernatant. Supernatant was collected and spun to equilibrium on 15–35% potassium tartrate gradients in TNE buffer, 200 mM NaCl, 50mM Tris-HCl [pH 7.4], 1mM EDTA, at 24,000 rpm in a Beckman SW-28 rotor overnight. The virus band was collected and used either for negative staining or to further purify on a linear 15–22% sucrose density gradient in the same buffer at 40,000 rpm in a Beckman SW-40Ti for 120 minutes. The entire sucrose gradient was collected in 0.5mL fractions and aliquots were counted by scintillation spectrometry for detection of labeled virus.

Transmission electron microscopy: monolayers

BHK cells were either transfected or infected with Sindbis virus (S420Y or Y180S/E183G) at an m.o.i. = 1. After a 1-h adsorption period, the inoculum was removed and fresh medium was added to the flasks. Incubation proceeded at 37°C for 16 h, after which supernatant was collected for titration and the monolayers were fixed with 3% glutaraldehyde (Ladd Research Industries, Inc., Williston, VT) in 0.1M cacodylic acid (Ladd Research Industries, Inc.) buffer. After cells were washed 3 \times with 0.1 M cacodylic acid, the cells were stained with 2% osmium tetroxide in cacodylic buffer for 1 h. Cells were then washed as before and embedded in 2% agarose. The agarose containing the cell sample was then pre-stained with 1% uranyl acetate (Polaron Instruments, Inc, Hatfield, PA) overnight at 4°C. The samples were washed and carried through a dehydration series of ethanol. Infiltration proceeds in SPURR compound (LADD Research Industries, Inc.). Blocks were then trimmed and thick sections (1.0 μ m) obtained on an LKB NOVA Ultratome (Leica Microsystems, Inc. Deerfield, IL). Sections were stained with 1.0% Toluidine Blue in 2.5%

sodium carbonate, mounted on glass slide with Permount™ (VWR International, South Plainfield, NJ) and observed under the light microscope for evaluation of the sample. Ultrathin sections were then obtained and were stained with 5% uranyl acetate in distilled water for 60 minutes and in Reynolds lead citrate (lead nitrate, sodium citrate and sodium hydroxide) (Mallinkrodt Baker Inc., Paris, KY) for 4 minutes. The samples were examined at 80 kV in a JEOL JEM 100S transmission electron microscope.

Negative staining

Virus collected from potassium tartrate or sucrose density gradients was attached to carbon-coated grids, washed 3 times with sterile H₂O and negatively stained with 1% uranyl acetate.

Critical point drying

Virus from tartrate gradients was attached to carbon grids and washed as above. The grids were then placed in a grid holder for critical point drying (Ladd Research Industries, Inc.) and dehydrated through an alcohol series. The technique was then performed using a Tousimis PVT-3B critical point dryer with liquid CO₂ (Tousimis Research Corporation, Rockville, MD) as described previously (Coombs and Brown, 1987b). After drying, the grids were placed in a Denton DV-502 vacuum evaporator and virus was shadowed using a platinum:palladium (80:20) wire.

Proteinase K treatment

BHK cells were transfected with S420Y and Y180S/E183G Sindbis virus. Monolayers were harvested at 16 hpi, washed with PBS and fixed with 4% paraformaldehyde in phosphate buffer pH 7.2 with 2.5% w/v sucrose. Cells were washed 3× with 0.1 M cacodylate buffer and embedded in agarose 2%. Dehydration was performed with ethanol (30–100%) and the cells were then embedded in LR White (Ladd Research Industries, Inc.) with 2 changes of 1 h each and 1 last change overnight. Curing was performed at 60°C for 20 h. Ultrathin sections were incubated with 2 ng/μL Proteinase K (from Sigma Co., St Louis, MO) for 15 minutes, washed 3× with water and then stained with 5% uranyl acetate for 60 minutes.

Acknowledgments

The authors gratefully acknowledge the assistance of John Mackenzie and Valerie Knowlton of the NCSU Center for Electron Microscopy for their assistance with electron microscopy. This research was supported by Grant AI-42775 from the National Institutes of Health, by a grant from the Foundation For Research (Carson City, Nevada) and by funds from the North Carolina Agricultural Research

Service. Davis Ferreira is a Graduate Fellowship student from PDEE-CAPES (Brazil).

References

- Anderson, T.F., 1954. Preservation of structure in dried specimens. *Proc. 3rd Int. Cong. Electron Microscopy* London, 122–129.
- Anthony, R.P., Brown, D.T., 1991. Protein-protein interactions in an alphavirus membrane. *J. Virol.* 65 (3), 1187–1194.
- Anthony, R.P., Paredes, A.M., Brown, D.T., 1992. Disulfide bonds are essential for the stability of the Sindbis virus envelope. *Virology* 190 (1), 330–336.
- Bonatti, S., Migliaccio, G., Blobel, G., Walter, P., 1984. Role of signal recognition particle in the membrane assembly of Sindbis viral glycoproteins. *Eur. J. Biochem* 140 (3), 499–502.
- Brown, D.T., 1980. The Assembly of Alphaviruses. In: Schlesinger, R.W. (Ed.), *The Togaviruses*. Academic Press, NY, pp. 473–501.
- Brown, D.T., Gliedman, J.B., 1973. Morphological variants of Sindbis virus obtained from infected mosquito tissue culture cells. *J. Virol.* 12 (6), 1534–1539.
- Brown, D.T., Smith, J.F., 1975. Morphology of BHK-21 cells infected with Sindbis virus temperature-sensitive mutants in complementation groups D and E. *J. Virol.* 15, 1262–1266.
- Brown, D.T., Waite, M.R.F., Pfefferkorn, E.R., 1972. Morphology and Morphogenesis of Sindbis virus as seen with freeze-etching techniques. *J. Virol.* 10, 534–536.
- Carleton, M., Brown, D.T., 1996. Disulfide bridge-mediated folding of Sindbis virus glycoproteins. *J. Virol.* 70 (8), 5541–5547.
- Caspar, D.L.D., Klug, A., 1962. Physical principles in the construction of regular viruses. *Cold Spring Harbor Symp. Quant. Biol.* 27, 1–24.
- Cheng, R.H., Kuhn, R.J., Olsen, N., Rossman, M.G., Choi, H.-K., Smith, T.J., Baker, T.S., 1995. Nucleocapsid and glycoprotein organization in an enveloped virus. *Cell* 80, 621–630.
- Choi, H.K., Lee, S., Zhang, Y.P., McKinney, B.R., Wengler, G., Rossman, M.G., Kuhn, R.J., 1996. Structural analysis of Sindbis virus capsid mutants involving assembly and catalysis [published erratum appears in *J. Mol. Biol.* 1997 Feb 28; 266(3)633–4]. *J. Mol. Biol.* 262 (2), 151–167.
- Condreay, L.D., Brown, D.T., 1988. Suppression of RNA synthesis by a specific antiviral activity in Sindbis virus-infected *Aedes albopictus* cells. *J. Virol.* 62 (1), 346–348.
- Coombs, K., Brown, D.T., 1987a. Organization of the Sindbis virus nucleocapsid as revealed by bifunctional cross-linking agents. *J. Mol. Biol.* 195 (2), 359–371.
- Coombs, K., Brown, D.T., 1987b. Topological organization of Sindbis virus capsid protein in isolated nucleocapsids. *Virus Res.* 7 (2), 131–149.
- Forsell, K., Xing, L., Kozlovskaya, T., Cheng, R.H., Garoff, H., 2000. Membrane proteins organize a symmetrical virus. *Embo. J.* 19 (19), 5081–5091.
- Friedman, R.M., Levin, J.G., Grimley, P.M., Berezsky, I.K., 1972. Membrane-associated replication complex in arbovirus infection. *J. Virol.* 10 (3), 504–515.
- Froshauer, S., Kartenbeck, J., Helenius, A., 1988. Alphavirus RNA replicase is located on the cytoplasmic surface of endosomes and lysosomes. *J. Cell. Biol.* 107 (6 Pt 1), 2075–2086.
- Gaedigk-Nitschko, K., Schlesinger, M.J., 1991. Site-directed mutations in Sindbis virus E2 glycoprotein's cytoplasmic domain and the 6K protein lead to similar defects in virus assembly and budding. *Virology* 183 (1), 206–214.
- Garoff, H., Simons, K., 1974. Location of the spike glycoproteins in the Semliki Forest virus membrane. *Proc. Natl. Acad. Sci. USA* 71 (10), 3988–3992.
- Gliedman, J.B., Smith, J.F., Brown, D.T., 1975. Morphogenesis of Sindbis virus in cultured *Aedes albopictus* cells. *J. Virol.* 16 (4), 913–926.

- Grimley, P.M., Berezsky, I.K., Friedman, R.M., 1968. Cytoplasmic structures associated with an arbovirus infection: loci of viral ribonucleic acid synthesis. *J. Virol.* 2 (11), 1326–1338.
- Harrison, S.C., 1986. In: *The Togaviridae and Flaviviridae*. Plenum Press, New York, pp. 21–34.
- Lee, H., Brown, D.T., 1994. Mutations in an exposed domain of Sindbis virus capsid protein result in the production of noninfectious virions and morphological variants. *Virology* 202, 390–400.
- Lee, H., Ricker, P.D., Brown, D.T., 1994. The configuration of Sindbis virus envelope proteins is stabilized by the nucleocapsid protein. *Virology* 204 (1), 471–474.
- Lee, S., Owen, K.E., Choi, H.K., Lee, H., Lu, G., Wengler, G., Brown, D.T., Rossmann, M.G., Kuhn, R.J., 1996. Identification of a protein binding site on the surface of the alphavirus nucleocapsid and its implication in virus assembly. *Structure* 4 (5), 531–541.
- Liljestrom, P., Garoff, H., 1991. Internally located cleavable signal sequences direct the formation of Semliki Forest virus membrane proteins from a polyprotein precursor. *J. Virol.* 65, 147–154.
- Liu, N., Brown, D.T., 1993a. Phosphorylation dephosphorylation events play critical roles in Sindbis virus maturation. *Virology* 196, 703–711.
- Liu, N., Brown, D.T., 1993b. Transient translocation of the cytoplasmic (endo) domain of a type I membrane glycoprotein into cellular membranes. *J. Cell. Biol.* 120 (4), 877–883.
- Lopez, S., Yao, J.S., Kuhn, R.J., Strauss, E.G., Strauss, J.H., 1994. Nucleocapsid-glycoprotein interactions required for assembly of alphaviruses. *J. Virol.* 68 (3), 1316–1323.
- Luo, T., Brown, D.T., 1994. A 55-kDa protein induced in *Aedes albopictus* (mosquito) cells by antiviral protein. *Virology* 200 (1), 200–206.
- Miller, M.L., Brown, D.T., 1993. The distribution of Sindbis virus proteins in mosquito cells as determined by immunofluorescence and immunoelectron microscopy. *J. Gen. Virol.* 74 (Pt 2), 293–298.
- Mulvey, M., Brown, D.T., 1994. Formation and rearrangement of disulfide bonds during maturation of the Sindbis virus E1 glycoprotein. *J. Virol.* 68 (2), 805–812.
- Paredes, A.M., Brown, D.T., Rothnagel, R., Chiu, W., Schoepp, R.J., Johnston, R.E., Prasad, B.V., 1993. Three-dimensional structure of a membrane-containing virus. *Proc. Natl. Acad. Sci. USA* 90 (19), 9095–9099.
- Paredes, A.M., Simon, M.N., Brown, D.T., 1992. The mass of the Sindbis virus nucleocapsid suggests it has $T = 4$ icosahedral symmetry. *Virology* 187 (1), 329–332.
- Pletnev, S.V., Zhang, W., Mukhopadhyay, S., Fisher, B.R., Hernandez, R., Brown, D.T., Baker, T.S., Rossmann, M.G., Kuhn, R.J., 2001. Locations of carbohydrate sites on alphavirus glycoproteins show that E1 forms an icosahedral scaffold. *Cell* 105 (1), 127–136.
- Rice, C.M., Levis, R., Strauss, J.H., Huang, H.V., 1987. Production of infectious RNA transcripts from Sindbis virus cDNA clones: mapping of lethal mutations, rescue of a temperature-sensitive marker, and in vitro mutagenesis to generate defined mutants. *J. Virol.* 61 (12), 3809–3819.
- Skoging-Nyberg, U., Liljestrom, P., 2001. M-X-I motif of semliki forest virus capsid protein affects nucleocapsid assembly. *J. Virol.* 75 (10), 4625–4632.
- Strauss, E.G., 1978. Mutants of Sindbis virus. III. Host polypeptides present in purified HR and ts103 virus particles. *J. Virol.* 28 (2), 466–474.
- Strauss, E.G., Birdwell, C.R., Lenches, E.M., Staples, S.E., Strauss, J.H., 1977. Mutants of Sindbis virus. II. Characterization of a maturation-defective mutant, ts103. *Virology* 82 (1), 122–149.
- Strauss, J.H., Strauss, E.G., 1994. The alphaviruses: gene expression, replication, and evolution. *Micro. Rev.* 58, 491–562.
- Tellinghuisen, T.L., Hamburger, A.E., Fisher, B.R., Ostendorp, R., Kuhn, R.J., 1999. In vitro assembly of alphavirus cores by using nucleocapsid protein expressed in *Escherichia coli*. *J. Virol.* 73 (7), 5309–5319.
- Tellinghuisen, T.L., Kuhn, R.J., 2000. Nucleic acid-dependent cross-linking of the nucleocapsid protein of Sindbis virus. *J. Virol.* 74 (9), 4302–4309.
- Tellinghuisen, T.L., Perera, R., Kuhn, R.J., 2001. In vitro assembly of Sindbis virus core-like particles from cross-linked dimers of truncated and mutant capsid proteins. *J. Virol.* 75 (6), 2810–2817.
- Von Bonsdorff, C.H., Harrison, S.C., 1978. Sindbis virus glycoproteins form a regular icosahedral surface lattice. *J. Virol.* 28, 578.
- Walker, D.H., Jr., Anderson, T.F., 1970. Morphological variants of coliphage ϕ 1. *J. Virol.* 5 (6), 765–782.
- Williams, R.C., Smith, K.M., 1958. The polyhedral form of the Tipula iridescent virus. *Biochim. Biophys. Acta* 28, 464–469.
- Wirth, D.F., Lodish, H.F., Robbins, P.W., 1979. Requirements for the insertion of the Sindbis envelope glycoproteins into the endoplasmic reticulum membrane. *J. Cell. Biol.* 81 (1), 154–162.
- Zhang, W., Fisher, B.R., Olson, N.H., Strauss, J.H., Kuhn, R.J., Baker, T.S., 2002. Aura virus structure suggests that the $T = 4$ organization is a fundamental property of viral structural proteins. *J. Virol.* 76 (14), 7239–7246.